Path integrals in the symbol space of chaotic mappings

1995 J. Phys. A: Math. Gen. 28 1889

(http://iopscience.iop.org/0305-4470/28/7/012)

J. Phys. A: Math. Gen. 28 (1995) 1889–1907. Printed in the UK

Path integrals in the symbol space of chaotic mappings

Christian Beck† and Tamás Tél‡

† School of Mathematical Sciences, Queen Mary and Westfield College, University of London, Mile End Road, London E1 4NS, UK

‡ Institute for Theoretical Physics, Eötvös University, Puskin u. 5-7, H-1088 Budapest, Hungary

Received 19 October 1994

Abstract. We introduce a path-integral-like partition function for chaotic mappings. This path integral is based on arbitrary non-Markovian stochastic processes generated by the symbolic dynamics of the map rather than the Wiener process. Our approach can be regarded as an extension of the thermodynamic formalism to infinitely many inverse temperatures. The concept of Rényi entropies is generalized to entropy functionals. A generalized transfer operator is introduced, which allows us to calculate the entropy functionals with high numerical precision. Several examples are worked out in detail.

1. Introduction

The symbolic dynamics technique has proved to be very useful for the qualitative and quantitative analysis of chaotic motion [1–4]. Regarding the initial values as random variables, deterministic chaotic systems generate complicated stochastic processes, which typically are neither Markovian nor Gaussian. A useful tool is to characterize these processes by a grammar of allowed and forbidden sequences in the symbol space, and to study the probabilities associated with the various symbol sequences. Indeed, the hierarchy of all probabilities yields quite a complete description of the stochastic properties of the dynamics.

The idea of the present paper is to use the complicated stochastic processes generated by nonlinear dynamical systems for the definition of a generalized path integral. The usual path integral, of utmost interest in Euclidean quantum theory and quantum field theory [5–7], is based on a simple Gaussian Markov process: the Wiener process, or Brownian motion. Nevertheless, replacing the Wiener process by a more complicated chaotic process, we can formally define a more general path integral. A particularly straightforward and easy method to introduce such a chaotic path integral is to choose a symbolic dynamical description, and to define a path integral in the symbol space, where transition probabilities are well defined. In contrast to the Markovian Wiener process, the transition probabilities will now also contain higher-order memory effects, due to the underlying deterministic chaotic dynamics.

Our path-integral approach can be formulated in an elegant way using the language of the thermodynamic formalism of dynamical systems [4, 8–14]. We consider partition functions where a suitable observable depends on the entire symbolic path of the chaotic system. In particular, we will choose an observable that measures the information production of the system in quite a general way. In the language of the thermodynamic formalism our approach means that we do not consider a single inverse temperature β but introduce an infinite sequence of different inverse temperatures $\beta_0, \beta_1, \beta_2, \ldots$. In the continuum limit

0305-4470/95/071889+19$19.50

these various inverse temperatures define an inverse temperature *field* (or a temperature function). In this way we will generalize the concept of Rényi entropies [15] to entropy *functionals*, which depend on a given test function, the temperature field.

It is well known that a stochastic process is not fully described by the moments (the characteristic function) alone, rather, its complete determination requires the knowledge of the set of all higher-order correlation functions (the characteristic functional) [16]. In the same context we claim that the most complete description of the information production of a chaotic system is not given by the Rényi entropies alone, but by the entropy functionals introduced here. The Rényi entropies are recovered from the entropy functionals for the special case of a constant test function.

Only in very rare cases can one evaluate path integrals in the symbol space (or entropy functionals) exactly. As one of these rare examples, we will treat symmetric and asymmetric tent maps, where we obtain explicit expressions for the functionals. In more general cases (m-step memory maps), a powerful numerical tool for the evaluation of entropy functionals is a generalized transfer matrix method. The generalized transfer matrices depend on the local temperature field. They reduce to the ordinary transfer matrices for a constant temperature field. The entropy functional is obtained from the growth rate of the product of local transfer matrices. The concept can be generalized to a path-integral transfer operator for general one-dimensional mappings.

This paper is organized as follows. In section 2 we introduce path integrals in the symbol space, starting from the definition of the usual path integral and generalizing to non-Markovian symbolic stochastic processes. In section 3 we introduce entropy functionals, which can be regarded as special path integrals in the symbol space, where the path-dependent observable is chosen in such a way that the information production of the system is measured. In section 4 we treat symmetric and asymmetric tent maps as simple examples. In section 5 processes with a two- and three-step memory are investigated, and the generalized transfer matrix is written down. Some numerical results are presented. In section 6 we generalize to m-step memory maps, as well as to maps with escape, and to non-hyperbolic cases. The general path-integral transfer operator is introduced in section 7. Our concluding remarks are given in section 8.

2. Path integrals in the symbol space

Let us first recall the definition of the usual path integral based on the Wiener process [5–7]. Given some observable A depending on the entire trajectory of the system, the path integral Z with respect to A is defined as

$$Z = \lim_{N\to\infty} Z_N \tag{1}$$

where

$$\begin{aligned} Z_N[A] = \int \mathrm{d}x_0 \int \mathrm{d}x_1 \ldots \int \mathrm{d}x_N \, p(x_N|x_{N-1}) p(x_{N-1}|x_{N-2}) \ldots \\ \ldots p(x_1|x_0) A(x_0, x_1, \ldots, x_N) \, . \end{aligned} \tag{2}$$

Here

$$p(x_k|x_{k-1}) = \frac{1}{\sqrt{2\pi D\tau}} \exp\left\{ -\frac{(x_k - x_{k-1})^2}{2D\tau} \right\} \tag{3}$$

are the transition probability densities of the Wiener process with diffusion constant D, and τ is a small time constant that goes to zero as N, the number of lattice points, approaches infinity:

$$\tau = \frac{t}{N} \tag{4}$$

where t is the total time elapsed. For example, to simulate a quantum system with potential V in Euclidean time t (obtained by Wick rotation $\tilde{t} \to i\tilde{t}$ of the physical time $\tilde{t}$) one chooses for the observable A

$$A(x_0, \ldots, x_N) = \exp\left\{-\frac{\tau}{\hbar} \sum_{k=0}^{N} V(x_k)\right\} \tag{5}$$

and $D = \hbar/m$ (see, for example, [14]). According to the Feynman–Kac formula, the integral Z_N converges to the integrated Euclidean propagator of the quantum system in the limit $N \to \infty$.

Let us now proceed to a chaotic mapping $f : X \to X$. We assume that a generating partition $B = (B_1, \ldots, B_R)$ of the phase space X exists (otherwise a supremum over all possible partitions has to be taken). The symbolic dynamics technique can then easily be applied (see, for example, [2, 4]). To each orbit $x_{k+1} = f(x_k)$ we associate the symbol sequence $i_0, i_1, i_2, \ldots,$ where $i_k = j$ if $x_k \in B_j$. Let us denote the probability to observe the symbol sequence $i_0, \ldots, i_N$ by $p(i_0, \ldots, i_N)$. Trajectories whose first symbols are $i_0, \ldots, i_N$ start from an interval $J^{(N+1)}(i_0, \ldots, i_N)$ called a level-$(N+1)$ cylinder. The probability $p(i_0, \ldots, i_N)$ is related to a given measure ν and the level-$(N+1)$ cylinders $J^{(N+1)}(i_0, \ldots, i_N)$ of the map by

$$p(i_0, \ldots, i_N) = \int_{J^{(N+1)}(i_0,\ldots,i_N)} \mathrm{d}\nu(x)\,. \tag{6}$$

Typically, one chooses ν to be either the natural invariant measure μ or the Lebesgue measure L. We can always factorize the probability $p(i_0, \ldots, i_N)$ into a product of conditional probabilities:

$$p(i_0, \ldots, i_N) = p(i_0)p(i_1|i_0)p(i_2|i_0, i_1)\ldots p(i_N|i_0, \ldots, i_{N-1})\,. \tag{7}$$

Here $p(i_k|i_0, \ldots, i_{k-1})$ denotes the conditional probability to observe the symbol i_k if the sequence $i_0, \ldots, i_{k-1}$ was observed before:

$$p(i_k|i_0, \ldots, i_{k-1}) = \frac{p(i_0, \ldots, i_k)}{p(i_0, \ldots, i_{k-1})} \tag{8}$$

(provided $p(i_0, \ldots, i_{k-1}) \neq 0$). Next, we define a partition function $Z_N^{(\nu)}$ for a given observable A and a measure ν in an analogous way as it is done for the 'classical' path integral

$$Z_N^{(\nu)}[A] = \sum_{i_0,\ldots,i_N} p(i_0)p(i_1|i_0)p(i_2|i_0, i_1)\ldots p(i_N|i_0, \ldots, i_{N-1})A(i_0, \ldots, i_N)\,. \tag{9}$$

The integrals over the continuous states are replaced by sums over the discrete states i_k. The fundamental difference compared to the usual path integral is the fact that, in general, for a chaotic mapping f, the transition probabilities $p(i_k|i_0, \ldots, i_{k-1})$ depend on the entire history $i_0, \ldots, i_{k-1}$. Generically, the stochastic processes generated by chaotic mappings are non-Markovian. Moreover, they are non-Gaussian. This is what makes the partition function (9) an interesting object to study in the thermodynamic limit $N \to \infty$.

If there is no generating partition, we either have to take a supremum over all possible partitions or introduce an additional continuum limit in (9), where the size of all cells approaches zero. In the latter case we obtain a generalized path integral defined on a continuum of states. The advantage of a generating partition is that the continuum limit need not to be performed.

It depends on the question under consideration what kind of function is chosen for the observable $A(i_0, \ldots, i_N)$. If one is interested in a generalized quantum mechanics based on a more complicated stochastic process than the Wiener process, an appropriate choice is

$$A(i_0, \ldots, i_N) = \exp\left\{-\frac{\tau}{\hbar}\sum_{k=0}^{N} V(i_k)\right\} \tag{10}$$

where V is a potential defined on the coarse-grained phase space. A similar approach, based on two-dimensional maps f and a path integral defined in the phase space rather than the symbol space, has been shown to retain the usual quantum mechanics based on the Wiener process in an appropriate continuum limit of the partition [14]. In this paper, however, we would like to consider other test functions A that are motivated by the needs to characterize the information production of chaotic systems rather than by quantum mechanical applications. These test functions will lead to a generalization of the concept of Rényi entropies.

3. Entropy functionals

We choose a test function given by the conditional probabilities itself raised to different powers $\beta_k - 1$:

$$A(i_0, \ldots, i_N) = p(i_0)^{\beta_0 - 1} p(i_1|i_0)^{\beta_1 - 1} \ldots p(i_N|i_0, \ldots, i_{N-1})^{\beta_N - 1}. \tag{11}$$

That is to say, we study the partition function

$$Z_N^{(\nu)}(\beta_0, \ldots, \beta_N) = \sum_{i_0, \ldots, i_N} p(i_0)^{\beta_0} p(i_1|i_0)^{\beta_1} \ldots p(i_N|i_0, \ldots, i_{N-1})^{\beta_N}. \tag{12}$$

Using equation (8), we may equivalently write

$$Z_N^{(\nu)}(\beta_0, \ldots, \beta_N) = \sum_{i_0, \ldots, i_N} p(i_0)^{q_0} p(i_0, i_1)^{q_1} \ldots p(i_0, \ldots, i_N)^{q_N} \tag{13}$$

$$q_k = \beta_k - \beta_{k+1} \qquad k = 0, \ldots, N-1 \tag{14}$$

$$q_N = \beta_N\,. \tag{15}$$

In the thermodynamic formalism, the β_j can be regarded as inverse temperatures. Usually one studies only one inverse temperature or at best two [17–22]. Here we want to illustrate that, in fact, the generalization to infinitely many inverse temperatures makes sense for a more general characterization of the information production of chaotic systems.

First of all, let us introduce conditional dynamical scaling indices α_k by writing

$$p(i_k|i_0, \ldots, i_{k-1}) = e^{\alpha_k} \tag{16}$$

($p(i_0) = e^{\alpha_0}$). By subsequent differentiation of $Z_N^{(\nu)}(\beta_0, \ldots, \beta_N)$ we obtain the higher-order correlation functions of these scaling indices:

$$\frac{\partial^{n_0}}{\partial \beta_0^{n_0}} \cdots \frac{\partial^{n_N}}{\partial \beta_N^{n_N}} Z_N^{(\nu)}(\beta_0, \ldots, \beta_N)|_{\beta_0=\beta_1=\cdots=\beta_N=1} = \left\langle \alpha_0^{n_0} \alpha_1^{n_1} \ldots \alpha_N^{n_N} \right\rangle. \tag{17}$$

Here $\langle \cdots \rangle$ denotes the expectation value with respect to the path probabilities $p(i_0, \ldots, i_N)$. Next, we introduce a generalized thermodynamic potential $G^{(\nu)}(\beta_0, \beta_1, \ldots)$ as

$$G^{(\nu)}(\beta_0, \beta_1, \ldots) = -\lim_{N\to\infty} \frac{1}{N} \ln Z_N^{(\nu)}(\beta_0, \ldots, \beta_N)\,. \tag{18}$$

It is defined for a given infinite sequence of inverse temperatures $\beta_0, \beta_1, \ldots$.

For a classical path integral, the time difference τ between the transition steps approaches zero in the thermodynamic limit $N \to \infty$ (see equation (4)). It is actually convenient for partition functions in the symbol space as well to consider an analogous scaling limit of the time. We may assume that each iteration step of the map corresponds to a time unit τ that is related to the total number N of steps by

$$\tau = \frac{t}{N} . \tag{19}$$

The total time elapsed is $t = N\tau$. We then perform the limit $\tau \to 0$, $N \to \infty$ in such a way that $t = N\tau$ stays finite. Introducing some function $\beta(t')$ defined on the interval $[0, t]$, for each N the β_k may be chosen as

$$\beta_k = \beta(k\tau) = \beta(kt/N) \tag{20}$$

(the $\beta_k = \beta_k^{(N)}$ actually depend on two indices k and N, but usually we will suppress the index N). In the limit $N \to \infty$ we obtain a functional depending on the given test function $\beta(t')$:

$$G_t^{(\nu)}[\beta] = -\lim_{N\to\infty} \frac{1}{N} \ln Z_N^{(\nu)}(\{\beta(kt/N)\}) . \tag{21}$$

This functional plays an analogous role for the information production of a chaotic system as the characteristic functional does for the correlation functions of a stochastic process (see, for example, [16]).

By a trivial change of coordinates (i.e. choosing the test function $\tilde{\beta}(t') = \beta(t'/t)$ instead of $\beta(t')$) we can always reduce the problem to that of a test function defined on the unit interval [0, 1]. Thus from now on we will use the following definition of the functional:

$$G^{(\nu)}[\beta] = -\lim_{N\to\infty} \frac{1}{N} \ln Z_N^{(\nu)}(\beta(0), \beta(1/N), \ldots, \beta(1)) . \tag{22}$$

In what follows we shall mainly concentrate on the case that the path probabilities are taken with respect to the natural measure μ of the map, and suppress the superscript μ. If all β_k take on the same value β, we obtain (up to a trivial factor) the Rényi entropies [15] $K(\beta)$:

$$G(\beta, \beta, \ldots) = (\beta - 1)K(\beta) . \tag{23}$$

For non-constant β_k, we obtain more general types of entropies characterizing the system in such a way that higher-order correlations in the symbol sequences are 'scanned' by the various β_k. $G(\beta_0, \beta_1, \ldots)$, respectively $G[\beta]$, will therefore be called the entropy functional.

What is the 'physical meaning' of these entropy functionals? Suppose we want to investigate the information production of the chaotic system in a time-dependent way. For example, we may first be more interested in topological properties of the symbolic trajectory ($\beta = 0$), but at the end of the observation (at time $t = 1$) be more interested in metric properties ($\beta = 1$). This change of interest can be modelled by some function $\beta(t)$ on the unit interval that increases from 0 to 1. The corresponding information production of the system is measured by $G[\beta]$. The result depends on the entire function $\beta(t)$. We will work out several examples in the following sections.

4. Symmetric and asymmetric tent maps

As a rather trivial example, let us first consider the symmetric tent map

$$f(x) = \begin{cases} 2x & x \leqslant \frac{1}{2} \\ 2(1-x) & x > \frac{1}{2} \end{cases} \tag{24}$$

on $X = [0, 1]$. Here the symbols i_k take on two values 0 and 1. We have $p(i_0, \ldots, i_N) = 2^{-(N+1)}$ and $p(i_k|i_0, \ldots i_{k-1}) = \frac{1}{2}$. Thus

$$Z_N(\beta_0, \ldots, \beta_N) = 2^{N+1}\left(\tfrac{1}{2}\right)^{\beta_0+\cdots+\beta_N} \tag{25}$$

(the same simple result applies to the binary shift map). This yields

$$G(\beta_0, \beta_1, \ldots) = \left(-1 + \lim_{N\to\infty} \frac{1}{N}(\beta_0 + \cdots + \beta_N)\right) \ln 2 . \tag{26}$$

Since $\beta_k = \beta(k\tau)$ and $1/N = \tau$, the entropy functional is given by

$$G[\beta] = \left(-1 + \int_0^1 \mathrm{d}t\, \beta(t)\right) \ln 2 . \tag{27}$$

For $\beta(t) = \beta_0 =$ constant this reduces to the well known result

$$G(\beta_0) = (-1 + \beta_0) \ln 2 \tag{28}$$

i.e. the Rényi entropies $K(\beta_0)$ have the constant value $\ln 2$. If the function $\beta(t)$ is not constant but increases (for example) as a power law in t from 0 to 1

$$\beta(t) = t^\eta \qquad \eta > 0 \tag{29}$$

we get

$$G[t^\eta] = -\frac{\eta}{\eta+1} \ln 2 \tag{30}$$

i.e. some intermediate value between $G(0) = -\ln 2$ and $G(1) = 0$, which depends on the exponent η.

A somewhat less trivial example is provided by the asymmetric tent map

$$f(x) = \begin{cases} x/w_0 & 0 \leqslant x \leqslant w_0 \\ (1-x)/w_1 & w_0 < x \leqslant 1 \end{cases} \tag{31}$$

on $X = [0, 1]$, where $w_1 = 1 - w_0$. In this case the natural measure has a constant density and, therefore, the probability to find a symbol sequence $i_0, \ldots, i_k$ is

$$p(i_0, \ldots, i_k) = w_{i_0} w_{i_1} \ldots w_{i_k} . \tag{32}$$

From equation (13) we obtain

$$Z_N(\beta_0, \ldots, \beta_N) = \sum_{i_0,\ldots,i_N} w_{i_0}^{q_0} (w_{i_0} w_{i_1})^{q_1} \ldots (w_{i_0} \ldots w_{i_N})^{q_N} . \tag{33}$$

Since $q_k + q_{k+1} + \cdots + q_N = \beta_k$,

$$Z_N(\beta_0, \ldots, \beta_N) = \sum_{i_0,\ldots,i_N} w_{i_0}^{\beta_0} w_{i_1}^{\beta_1} \ldots w_{i_N}^{\beta_N} \tag{34}$$

$$= \prod_{k=0}^{N} \left(w_0^{\beta_k} + w_1^{\beta_k}\right) . \tag{35}$$

This yields

$$G(\beta_0, \beta_1, \ldots) = -\lim_{N\to\infty} \frac{1}{N} \sum_{k=0}^{N} \ln\left(w_0^{\beta_k} + w_1^{\beta_k}\right) \tag{36}$$

and the entropy functional is given by

$$G[\beta] = -\int_0^1 \mathrm{d}t \, \ln\left(w_0^{\beta(t)} + w_1^{\beta(t)}\right). \tag{37}$$

Recently, it has been shown that the asymmetric tent map produces information in just the same way as successive measurements on a quantum mechanical system with a finite two-dimensional phase space do [23]. In this physical application, a non-constant $\beta(t)$ (or in general, a test function depending on the entire symbolic trajectory) corresponds to a measuring device that changes in time.

5. Processes with two- and three-step memories

The asymmetric tent map provides an example for which the conditional probabilities only depend on the very last digit of the symbolic code. One can extend the range of the memory by one step if one considers piecewise linear single humped maps that have breakpoints (i.e. non-differentiable points) at the two pre-images of their maxima, too (see figure 1). Such maps are linear on their level-2 cylinders $J^{(2)}(i_0, i_1)$ (in the case of fully developed maps, like, for example, the one shown in figure 1, only three of the slopes are independent). In such cases the density $\varrho(x)$ of the natural measure μ is piecewise constant on the two level-1 cylinders. Let $s(i_0, i_1)$ denote the modulus of the slope on cylinder $J^{(2)}(i_0, i_1)$. The ratio of the constant values $\varrho(0)$ and $\varrho(1)$ on $J^{(1)}(0)$ and $J^{(1)}(1)$, respectively, follows from the Frobenius–Perron equation

$$\varrho(0) = \varrho(0)/s(00) + \varrho(1)/s(10) \tag{38}$$

$$\varrho(1) = \varrho(0)/s(01) + \varrho(1)/s(11) \tag{39}$$

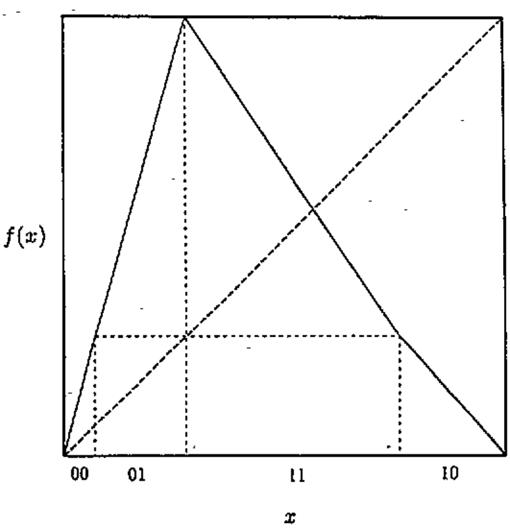

Figure 1. Example of a two-step memory map on $X = [0, 1]$. The parameters are $s(0, 0) = 4$, $s(0, 1) = \frac{7}{2}$, $s(1, 1) = \frac{3}{2}$, $s(1, 0) = \frac{8}{7}$ and $l(0, 0) = \frac{2}{29}$, $l(0, 1) = \frac{6}{29}$, $l(1, 1) = \frac{14}{29}$, $l(1, 0) = \frac{7}{29}$. The general condition for the Markov property of such maps implies the relation $s(0, 1)s(1, 0)(s(0, 0) - 1)(s(1, 1) - 1) = s(0, 0)s(1, 1)$ between the slopes. The length scales follow from normalization.

(see, for example, [24]). The one-symbol probabilities are then obtained as $p(i_0) = \varrho(i_0)l(i_0)$. Here and in what follows we use the notation that $l(i_0, i_1, \ldots, i_{N-1})$ denotes the length of the level-N cylinder $J^{(N)}(i_0, i_1, \ldots, i_{N-1})$.

A direct computation of the two-symbol partition sum shows that Z_1 is the scalar product of two real vectors

$$Z_1(\beta_0, \beta_1) = \langle c(\beta_1)|a(\beta_1, \beta_0)\rangle \tag{40}$$

where the components of a and c are

$$\langle a(\beta, \beta')|i_0\rangle = p^{\beta'}(i_0)l^{-\beta}(i_0) \tag{41}$$

and

$$\langle c(\beta)|i_0\rangle = l^{\beta}(i_0, 0) + l^{\beta}(i_0, 1) \tag{42}$$

respectively ($i_0 = 0, 1$). We use the convention that 'ket's denote column vectors.

In the case of symbol sequences of length three, a 2×2 matrix T is sandwiched between the vectors a and c:

$$Z_2(\beta_0, \beta_1, \beta_2) = \langle c(\beta_2)|T(\beta_2, \beta_1)|a(\beta_1, \beta_0)\rangle \tag{43}$$

where

$$\langle i|T(\beta, \beta')|i'\rangle = l^{\beta'-\beta}(i', i)s^{-\beta}(i', i)\,. \tag{44}$$

Note that the argument of c has been shifted to β_2.

Considering longer and longer symbols implies the appearance of more and more products of the same matrix T taken at different temperatures. One obtains

$$Z_N(\beta_0, \ldots, \beta_N) = \langle c(\beta_N)|T(\beta_N, \beta_{N-1})\ldots T(\beta_2, \beta_1)|a(\beta_1, \beta_0)\rangle\,. \tag{45}$$

This form suggests that T can be called a *transfer matrix* which in our case also transfers the *temperature*. It is worth noting that transfer matrices of this kind have already been used in the theory of Ising systems a long time ago [25]. In fact, the two-step memory map shown in figure 1 corresponds to a nearest-neighbour Ising chain [26], and our computation is the analogue of applying the transfer matrix method to a chain the temperature of which is changing in the course of this procedure. It also follows from (18) that the entropy functional $G(\beta_0, \beta_1, \ldots)$ can be obtained from the asymptotic *growth rate* of the $(N-1)$-fold matrix product $T(\beta_N, \beta_{N-1})\ldots T(\beta_2, \beta_1)$ acting on any fixed generic vector.

In order to find the general structure of the transfer matrix let us also consider cases with three-step memories. Such maps can be obtained by introducing breakpoints at the endpoints of the level-3 cylinders, too. Let $s(i_0, i_1, i_2)$ denote the modulus of the slope of the piecewise linear map on the cylinders $J^{(3)}(i_0, i_1, i_2)$ (see figure 2).

The natural density now turns out to be piecewise constant on the level-2 cylinders. Denoting its values by $\varrho(i_0, i_1)$, the Frobenius–Perron equation implies that the column vector $|\varrho\rangle = (\varrho(0,0), \varrho(0,1), \varrho(1,1), \varrho(1,0))$ is a solution of the matrix equation $|\varrho\rangle = T|\varrho\rangle$ where T is

$$T = \begin{pmatrix} s^{-1}(0,0,0) & 0 & 0 & s^{-1}(1,0,0) \\ s^{-1}(0,0,1) & 0 & 0 & s^{-1}(1,0,1) \\ 0 & s^{-1}(0,1,1) & s^{-1}(1,1,1) & 0 \\ 0 & s^{-1}(0,1,0) & s^{-1}(1,1,0) & 0 \end{pmatrix}. \tag{46}$$

With the knowledge of ϱ one can compute the cylinder measures and the conditional probabilities of symbol sequences of any length. A direct computation of the partition sum then leads to the form

$$Z_N(\beta_0, \ldots, \beta_N) = \langle c(\beta_N)|T(\beta_N, \beta_{N-1})\ldots T(\beta_3, \beta_2)|a(\beta_2, \beta_1, \beta_0)\rangle\,. \tag{47}$$

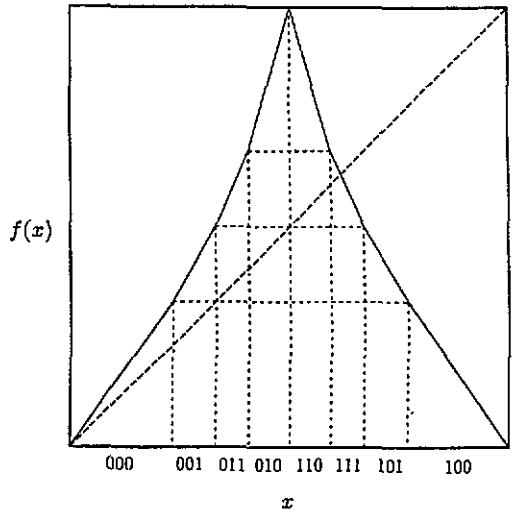

Figure 2. Example of a three-step memory map on $X = [0, 1]$. For simplicity, we have chosen a symmetric case, although our approach is valid in full generality. The parameters are $s(0,0,0) = \frac{10}{7}$, $s(0,0,1) = \frac{12}{7}$, $s(0,1,1) = \frac{9}{4}$, $s(0,1,0) = \frac{7}{2}$ and $l(0,0,0) = \frac{49}{212}$, $l(0,0,1) = \frac{21}{212}$, $l(0,1,1) = \frac{16}{212}$, $l(0,1,0) = \frac{20}{212}$. The general condition for the Markov property of such maps implies the relation $s(0,0,1)\,s(0,1,0)\,(s(0,0,0)-1)(s(0,1,1)-1) = s(0,0,0)s(0,1,1)$ between the slopes. The length scales follow from normalization.

Now the vectors a and c can be expressed as

$$\langle a(\beta,\beta',\beta'')|i_0,i_1\rangle = p^{\beta''}(i_0)p^{\beta'}(i_1|i_0)l^{-\beta}(i_0,i_1) \tag{48}$$

$$\langle c(\beta)|i_0,i_1\rangle = l^{\beta}(i_0,i_1,0) + l^{\beta}(i_0,i_1,1)\,. \tag{49}$$

The transfer matrix is a 4×4 matrix with eight non-zero elements and depends on two consecutive values of β just as in the previous case. It is of the form

$$T(\beta,\beta') = \begin{pmatrix} \frac{l^{\beta'-\beta}(0,0,0)}{s^{\beta}(0,0,0)} & 0 & 0 & \frac{l^{\beta'-\beta}(1,0,0)}{s^{\beta}(1,0,0)} \\ \frac{l^{\beta'-\beta}(0,0,1)}{s^{\beta}(0,0,1)} & 0 & 0 & \frac{l^{\beta'-\beta'}(1,0,1)}{s^{\beta}(1,0,1)} \\ 0 & \frac{l^{\beta'-\beta}(0,1,1)}{s^{\beta}(0,1,1)} & \frac{l^{\beta'-\beta}(1,1,1)}{s^{\beta}(1,1,1)} & 0 \\ 0 & \frac{l^{\beta'-\beta}(0,1,0)}{s^{\beta}(0,1,0)} & \frac{l^{\beta'-\beta}(1,1,0)}{s^{\beta}(1,1,0)} & 0 \end{pmatrix}. \tag{50}$$

This is exactly of the same structure as the usual transfer matrix introduced in the thermodynamic formalism of dynamical systems [27]. Note that $T(\beta,\beta')$ contains geometrical factors solely, and the only place where the densities appear is in the vector a. The matrix representing the Frobenius–Perron equation is just $T = T(1,1)$.

The generalized transfer matrix method provides us with a very precise algorithm to calculate entropy functionals numerically. To test our method, we have chosen three different test functions $\beta(t)$ on $[0,1]$ parametrized by a parameter η, namely $\beta_\eta^{(1)}(t) = t^\eta$, $\beta_\eta^{(2)}(t) = \eta\sin 2\pi t$, and $\beta_\eta^{(3)}(t) = \eta t$. The β values tested by these functions take values around the origin. By adding arbitrary constants or taking other functional forms any subset of the β-axis can be investigated. We have chosen four different examples of mappings: The symmetric tent map, an asymmetric tent map with $w_0 = \frac{1}{6}$, a two-step memory map with $s(0,0) = 4$, $s(0,1) = \frac{7}{2}$, $s(1,1) = \frac{3}{2}$, $s(1,0) = \frac{8}{7}$ (figure 1), and a symmetric three-step memory map with $s(0,0,0) = \frac{10}{7}$, $s(0,0,1) = \frac{12}{7}$, $s(0,1,1) = \frac{9}{4}$, $s(0,1,0) = \frac{7}{2}$ (figure 2). The entropy functional has been calculated numerically from the asymptotic growth rate of the partition function (45), where the transfer matrix is given by (44) and (50), respectively. The numerical results for $G[\beta_\eta^{(i)}]$ as a function of the parameter η are plotted in figures 3–5. The convergence of the method is rapid and the necesssary amount of computing time is very small. Proceeding to just $N = 50$, we already obtain the entropy functionals $G[\beta_\eta^{(i)}]$ with a precison of five digits. This means that the errors in figures 3–5 are smaller than

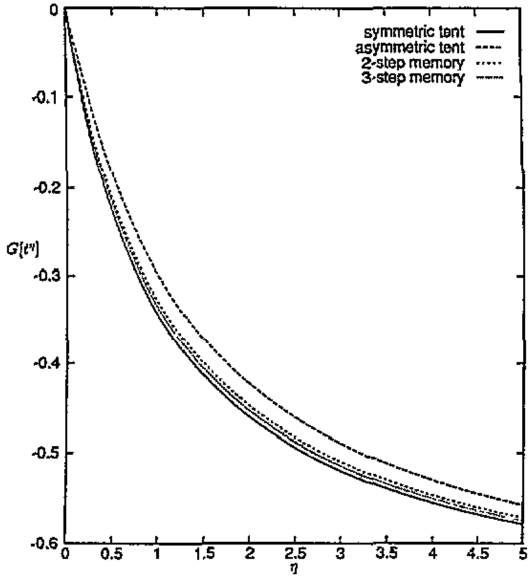

Figure 3. Entropy functionals obtained with the test function $\beta_\eta^{(1)}(t) = t^\eta$ for the symmetric tent map, the asymmetric tent map with $w_0 = 1/6$, and the two- and three-step memory maps of figure 1 and figure 2, respectively. Each curve starts in the origin because for $\beta \equiv 1$ the entropy functional vanishes. The range of β values tested is $[0, 1]$ in this case. For large η all curves come close to the horizontal line $G \equiv -\ln 2$ since then the function t^η takes on values very close to zero in almost the entire interval $0 < t < 1$, and for $\beta \equiv 0$ the modulus of the entropy function coincides with the topological entropy $K(0) = \ln 2$ of the map.

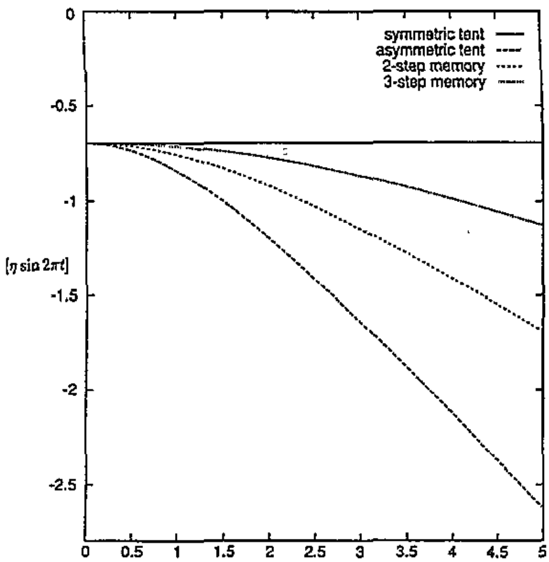

Figure 4. Same as figure 3, but with an oscillating test function with average 0 ($\beta_\eta^{(2)}(t) = \eta \sin 2\pi t$). The curves now start at $G = -K(0) = -\ln 2$. Note that the deviation from the entropy functional of the tent map increases with the amplitude η of the oscillations. The interval tested is now $[-\eta, \eta]$. The monotonic decrease of G with η follows from the observation that the contributions $(\beta - 1)K(\beta)$ related to the local Renyi entropies $K(\beta)$ are larger in modulus for $\beta < 0$ than for $\beta' = -\beta$.

the widths of the curves plotted. Most of our numerics was done with $N = 100$. The symmetric tent map mainly served us as an example to check our results, since for this special mapping all entropy functionals can be evaluated analytically with the help of (27):

$$G^{\text{tent}}[\beta_\eta^{(1)}] = -\frac{\eta}{\eta+1}\ln 2 \tag{51}$$

$$G^{\text{tent}}[\beta_\eta^{(2)}] = -\ln 2 \tag{52}$$

$$G^{\text{tent}}[\beta_\eta^{(3)}] = -\left(1-\tfrac{1}{2}\eta\right)\ln 2 \tag{53}$$

(the same formulae are valid for the binary shift map). The plots thus show in a quantitative way how the information productions of the various mappings deviate from that of a simple Bernoulli shift dynamics.

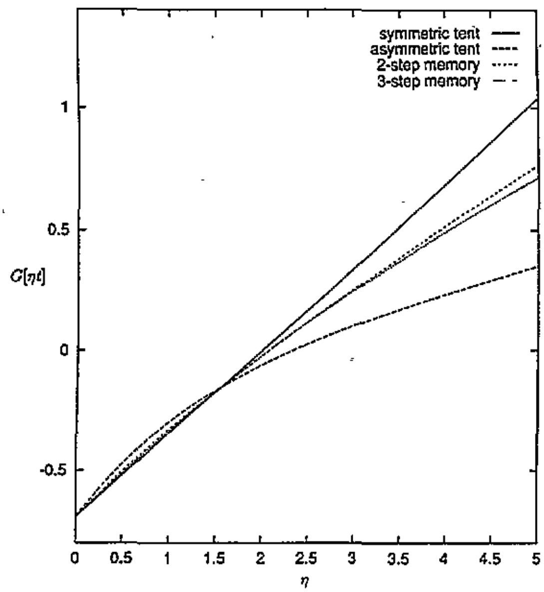

Figure 5. Same as figure 3, but with a linear test function $\beta_\eta^{(3)}(t) = \eta t$. The monotonic increase of G with η is due to the fact that the interval $[0, \eta]$ tested by ηt is non-negative. The local contributions $(\beta - 1)K(\beta)$ of increasing order become more and more dominating.

6. The general case

First, consider the case of an m-step memory map that is piecewise linear on its level-m cylinders. It is clear from the examples above that Z_N can then be written as

$$Z_N(\beta_0, \ldots, \beta_N) = \langle c(\beta_N)|T(\beta_N, \beta_{N-1})\ldots T(\beta_m, \beta_{m-1})|a(\beta_{m-1}, \ldots, \beta_0)\rangle \tag{54}$$

where a and c are now vectors with 2^{m-1} components and T is a $2^{m-1} \times 2^{m-1}$ matrix with 2^m non-zero elements. Their explicit forms can be derived in an analogous way as above.

Let us now turn to general smooth maps exhibiting fully developed chaos. The effect of truncating the memory in the symbol sequence distribution has been studied in detail. Szépfalusy and Györgyi pointed out [28] that truncated entropies computed with the assumption of having an l-step memory in $p(i_0, \ldots, i_N)$ approach the exact metric entropy $K(1)$ in an exponential way as $\exp(-\gamma l)$ where γ is a characteristic quantity of the map, the so-called entropy decay rate. It is typically of order unity with the exception of near-intermittent maps where γ is very small. In intermittent systems the decay is algebraic implying $\gamma = 0$. For one-dimensional fully developed maps the entropy decay rate can also be expressed by the order-3 Rényi entropy $K(3)$ as $\gamma = 2K(3)$. Analogous investigations of the order-q Renyi entropies $K(q)$ led to the introduction of generalized entropy decay rates $\gamma(q)$ [29]. They are typically of the same order of magnitude as γ. These results show that for fixed β values memory effects are only important for sequence lengths of the order of $1/\gamma$. In our path-integral approach, we thus expect that for functions testing a not too broad range of β, smooth maps behave similarly as $m \approx 1/\gamma$-step piecewise linear models, and with the exception of near-intermittent cases this m is of order unity.

As an example, we calculated entropy functionals for l-step memory approximations of the fully developed logistic map $f(x) = 4x(1-x)$. These piecewise linear approximations are obtained by attributing constant slopes to the N-cylinders of f. A straightforward calculation yields for the two-step memory approximation the slopes $s(00) = s(10) = \sqrt{2}(\sqrt{2}+1)$, $s(01) = s(11) = \sqrt{2}$, and for the three-step memory approximation $s(000) = s(100) = 2 + \sqrt{2+\sqrt{2}}$, $s(001) = s(101) = \sqrt{2} + \sqrt{2+\sqrt{2}}$, $s(011) = s(111) = \sqrt{2} + \sqrt{2-\sqrt{2}}$, $s(010) = s(110) = \sqrt{2-\sqrt{2}}$. Figure 6 shows the corresponding entropy functionals for the same test functions $\beta_\eta^{(i)}(t)$ as in figures 3–5. Indeed, for $\eta \leqslant 2$ there is hardly any difference between the results for the two- and three-step mappings, thus here the functionals approximate those of the logistic map quite precisely. On the other hand, for larger values of η, corresponding to larger β intervals tested, the difference between

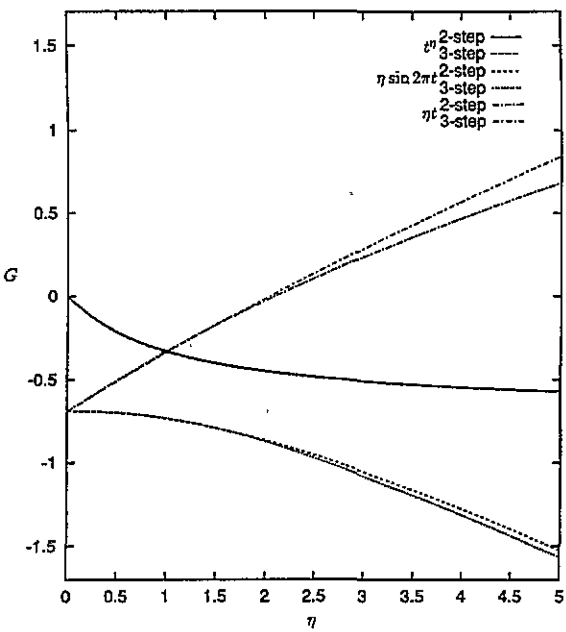

Figure 6. Entropy functionals obtained for two- and three-step memory approximations of the fully developed logistic map $f(x) = 4x(1-x)$. The test functions are $\beta_\eta^{(1)}(t) = t^\eta$, $\beta_\eta^{(2)}(t) = \eta\sin(2\pi t)$, $\beta_\eta^{(3)}(t) = \eta t$, respectively. The entropy decay rate for this map is $\gamma = \ln 4$ [28]. Thus we expect that a three-step memory map is a good approximation. This is supported by the good coincidence of the two- and three-step results for those η values where the range of temperature tested is not too broad.

the two- and three-step functionals increases. Here memory effects are measured in a more sensitive way.

The natural measures of smooth hyperbolic maps have non-singular densities. Therefore, the scaling behaviour of the length scales and the cylinder measures is the same. Consequently, for such maps we expect Z_N to appear in the form of (55) where the transfer matrix is of the type

$$\langle i_1, i_2, \ldots, i_{m-1}|T(\beta, \beta')|i_0, i'_1, \ldots, i'_{m-2}\rangle \quad = t^{(\beta,\beta')}(i_0, \ldots i_{m-1})\delta_{i_1,i'_1} \ldots \delta_{i_{m-2},i'_{m-2}} . \tag{55}$$

The non-zero matrix elements are

$$t^{(\beta,\beta')}(i_0, \ldots i_{m-1}) = l^{\beta'-\beta}(i_0, \ldots i_{m-1})\sigma^{\beta}(i_0, \ldots, i_{m-1}) \tag{56}$$

where σ stands for the daughter-to-mother ratio [26] defined as

$$\sigma(i_0, \ldots, i_{m-1}) = \frac{l(i_0, \ldots, i_{m-1})}{l(i_1, \ldots, i_{m-1})} . \tag{57}$$

In piecewise linear m-step processes $\sigma(i_0, \ldots, i_{m-1}) = s^{-1}(i_0, \ldots, i_{m-1})$ and we recover the previous results. For general smooth hyperbolic maps the explicit form of the vectors a and c is not known but the generalized thermodynamic potential can be extracted from the growth rate of the product $T(\beta_N, \beta_{N-1}) \ldots T(\beta_m, \beta_{m-1})$ when acting on any generically chosen fixed vector c'. Defining

$$\lambda(\beta_0, \ldots, \beta_N) = \frac{\| T(\beta_N, \beta_{N-1}) \ldots T(\beta_{m-1}, \beta_m)|c'\rangle \|}{\| |c'\rangle \|} \tag{58}$$

as the growth rate of the product $T(\beta_N, \beta_{N-1}) \ldots T(\beta_m, \beta_{m-1})|c'\rangle$, we obtain

$$G(\beta_0, \beta_1, \ldots) = -\lim_{N\to\infty} \frac{1}{N} \ln \lambda(\beta_0, \ldots \beta_N) \tag{59}$$

independently of c'. Here $\| \, \|$ denotes the length (or any appropriate norm) of a vector. The formula can again be used for the numerical determination of the generalized thermodynamic potential by choosing e.g. $|c'\rangle$ as the vector $(1, \ldots, 1)$. In practice, one calculates numerically the difference $\ln \lambda(\beta_0^{(N)}, \ldots, \beta_N^{(N)}) - \ln \lambda(\beta_0^{(N+1)}, \ldots, \beta_{N+1}^{(N+1)})$, where $\beta_k^{(N)} = \beta(k/N)$. The difference approaches $G[\beta]$ for large N.

We emphasize again that the leading exponential behaviour is governed by the transfer matrix rather than by the vectors it is acting on. Vectors a and c in (55) contain information concerning the natural density but contribute to the prefactors only. This is why the generalized thermodynamic potential can be determined by any generic choice of c' correctly.

It is worth mentioning briefly the case of open maps generating transient chaos [30]. Such maps possess fractal invariant sets, and the cylinders provide an ever refining coverage of this set. Covering a set of measure zero, the total length of the level-N cylinders decreases exponentially with N. Therefore, what appears in such cases in the transfer matrix is the normalized length $l(i_0, \ldots, i_{m-1}) / \sum_{i_0,\ldots,i_{m-1}} l(i_0, \ldots, i_{m-1})$ rather than the length itself.

Finally, let us return to fully developed chaotic maps and investigate the effect of non-hyperbolicity. In such cases the natural density is no longer analytic and, because of its singularity, the cylinder measures $p(i_0, \ldots, i_N)$ are not always proportional to the cylinder lengths $l(i_0, \ldots, i_N)$. In order to define the entropy functional we have to use the probabilities instead of the lengths. Therefore, we define the transfer matrix in its most general form by replacing $t^{(\beta,\beta')}$ by

$$t_\mu^{(\beta,\beta')}(i_0, \ldots i_{m-1}) = p^{\beta'-\beta}(i_0, \ldots, i_{m-1})\sigma_\mu^{\beta}(i_0, \ldots, i_{m-1}) \tag{60}$$

where σ_μ denotes the daughter-to-mother ratio of the cylinder measures:

$$\sigma_\mu(i_0, \ldots, i_{m-1}) = \frac{p(i_0, \ldots, i_{m-1})}{p(i_1, \ldots, i_{m-1})}. \tag{61}$$

It has to be emphasized that the definition based on the length scales still remains meaningful but leads to a quantity different from that related to entropies. Consider the partition sum $Z_N^{(\mathrm{L})}$ obtained by replacing in (13) the symbol probabilities $p(i_0, i_1, \ldots)$ by the Lebesgue measure (length) $l(i_0, i_1, \ldots)$ of the cylinders. The corresponding thermodynamic potential $G^{(\mathrm{L})}(\beta_0, \beta_1, \ldots)$ differs from $G(\beta_0, \beta_1, \ldots)$ and corresponds in the limit of a homogenous temperature $\beta_i \equiv \beta$ to the so-called free energy $\beta F(\beta)$ [31, 12, 4] (or topological pressure) of the map: $G^{(\mathrm{L})}(\beta, \beta, \ldots) = \beta F(\beta)$. The length scale transfer matrix

$$\langle i_1, i_2, \ldots, i_{m-1}|T^{\mathrm{L}}(\beta, \beta')|i_0, i_1', \ldots, i_{m-2}'\rangle = t^{(\beta,\beta')}(i_0, \ldots i_{m-1})\delta_{i_1,i_1'} \ldots \delta_{i_{m-2},i_{m-2}'} \tag{62}$$

where t is given as in (55) and (56), yields the free energy functional $G^{(\mathrm{L})}$ as

$$G^{(\mathrm{L})}(\beta_0, \beta_1, \ldots) = -\lim_{N\to\infty} \frac{1}{N} \ln \lambda^{(\mathrm{L})}(\beta_0, \ldots \beta_N). \tag{63}$$

Here $\lambda^{(\mathrm{L})} = (\| T^{(\mathrm{L})}(\beta_N, \beta_{N-1}) \ldots T^{(\mathrm{L})}(\beta_m, \beta_{m-1})|c'\rangle \|)/(\| |c'\rangle \|)$.

7. The path-integral transfer operator

The essential difference between the transfer matrices introduced above and their traditional forms appearing in the thermodynamical formalism is the factor $l^{\beta_n-\beta_{n+1}}$ (or $p^{\beta_n-\beta_{n+1}}$) that becomes unity only for $\beta_n = \beta_{n+1}$. These factors can play an essential role in determining the entropy functionals for general temperature distributions $\beta(t)$. For example, a bivalued sequence $\beta_0, \beta_1, \beta_0, \beta_1 \ldots$, that leads to a nowhere differentiable function $\beta(t)$, defines an entropy functional $G(\{\beta_0, \beta_1\}) = -\ln \lambda^{1/2}(\beta_0, \beta_1)$ where $\lambda(\beta_0, \beta_1)$ is the largest eigenvalue of the matrix product $T(\beta_0, \beta_1)T(\beta_1, \beta_0)$.

The class of *smooth* temperature distributions is, however, special in the sense that in this case the factors $l^{\beta_n-\beta_{n+1}}$ (or $p^{\beta_n-\beta_{n+1}}$) do not contribute to the entropy functionals. Although factors $l^{\beta-\beta'}$ (or $p^{\beta-\beta'}$) with temperature differences of the order of unity appear in the products of transfer matrices, they are not growing exponentially with N and, therefore, do not contribute to the functional in (60), only modify the prefactors (for a rigorous proof, see the appendix). Thus, for smooth temperature distributions the transfer matrix (55)–(57) or (60) leads to the same functional as its simplified form obtained by formally setting $l(i_0, \ldots, i_{N-1}) \equiv 1$ or $p(i_0, \ldots, i_{N-1}) \equiv 1$ in the nominators. Consequently, it is sufficient to use products of the traditional transfer matrices $T(\beta) \equiv T(\beta, \beta' = \beta)$ taken at different temperatures. This leads to accurate results in the limit $N \to \infty$ (but has different finite-N corrections compared to the ones based on the exact transfer matrix). We notice that for smooth temperature fields only the local temperature β_k, but not the local temperature difference $\beta_k - \beta_{k+1}$ influences the generalized thermodynamic potential.

Recall that the traditional transfer matrix of a one-dimensional map $f(x)$ can be considered as the discretized version of a transfer operator $\mathcal{L}(\beta)$, sometimes also called the generalized Frobenius–Perron operator [32]. It acts on some function Q defined on the support X of maps f as

$$L(\beta)Q(y) = \sum_{x\in f^{-1}(y)} \frac{Q(x)}{|f'(x)|^\beta}. \tag{64}$$

In an appropriate class of smooth functions $Q(y)$, the free energy $\beta F(\beta)$, which for hyperbolic maps coincides with $(\beta - 1)K(\beta)$, is obtained as $-\ln \lambda(\beta)$ where $\lambda(\beta)$ is the largest eigenvalue of $\mathcal{L}(\beta)$ in this class.

In the same spirit, we claim that it makes sense to consider a 'path-integral transfer operator' $\mathcal{L}[\beta]$ defined for any *smooth* temperature distribution $\beta(t)$. Formally it is obtained by considering the $N \to \infty$ limit of operators $\mathcal{L}_N(\beta_0, \ldots, \beta_{N-1})$ acting on functions Q as

$$\mathcal{L}_N(\beta_0, \ldots, \beta_{N-1})Q(y) = \sum_{x_0 \in f^{-N}(y)} \frac{Q(x_0)}{|f'(x_0)|^{\beta_0} \ldots |f'(x_{N-1})|^{\beta_{N-1}}} \tag{65}$$

where $\beta_j = \beta(j/N)$ and x_l is the lth image $f^l(x_0)$ of x_0. Let $\lambda(\beta_0, \ldots, \beta_{N-1})$ denote the largest eigenvalue of $\mathcal{L}_N$ in the class of smooth functions. The entropy functional $G^{(\mathrm{L})}[\beta]$, which for hyperbolic maps coincides with $G[\beta]$, is then obtained as the $N \to \infty$ limit of $-1/N \ln \lambda$. In other words, we expect $\mathcal{L}_N Q(y)$ to behave for large N as $\exp(-G^{(\mathrm{L})}[\beta]N)$, i.e. to obtain $G^{(\mathrm{L})}$ as

$$G^{(\mathrm{L})}[\beta] = -\lim_{N\to\infty} \ln \frac{\mathcal{L}_{N+1}Q(y)}{\mathcal{L}_N Q(y)}. \tag{66}$$

The convergence in N is expected to be exponentially fast, and rather good results can be obtained by computing the largest eigenvalue numerically. On the other hand, when working out the action of $\mathcal{L}_N$ on a binary tree, one typically cannot go further than $N \approx 20$ because of storage limitations. At such values of N the discrete set of β_j does not yet yield a sufficiently good approximation to the smooth function $\beta(t)$. One should go up to $N = 50$ to get high accuracy just like in the transfer matrix case.

In order to illustrate the efficiency of the operator method, let us here consider a related problem, which is not tangled in any way by the covergence of the β_j to $\beta(t)$. Instead of a smooth test function $\beta(t)$ we take a given infinite sequence of parameters $\beta_0, \beta_1, \beta_2, \ldots$. If the sequence is *periodic* with period p, we define a thermodynamic potential $\tilde{G}^{(\mathrm{L})}$ by

$$\tilde{G}^{(\mathrm{L})}(\beta_0, \ldots, \beta_{p-1}) = -\frac{1}{p} \lim_{N\to\infty} \ln \frac{\mathcal{L}_{N+p}Q(y)}{\mathcal{L}_N Q(y)}. \tag{67}$$

Note that, in general, $\tilde{G}^{(\mathrm{L})}$ is not the same as the free energy functional $G^{(\mathrm{L})}$ because the factors $l^{\beta_n - \beta_{n+1}}$ or $p^{\beta_n - \beta_{n+1}}$ are now not negligible in the matrices (56) or (61). Nevertheless, we found it worth studying the potential $\tilde{G}^{(\mathrm{L})}$ related to the largest eigenvalue of $\mathcal{L}_N$ since it is another interesting characteristic quantity that can be attributed to any mapping.

As an example, we numerically determined $\tilde{G}^{(\mathrm{L})}(\beta_0, \beta_1)$ for the fully developed logistic map $f(x) = 4x(1-x)$ and a periodic sequence $\beta_0, \beta_1, \beta_0, \beta_1, \ldots$ of period 2. The results of our numerical calculation (based on equation (67)) are plotted in figure 7. On the diagonal $\beta_0 = \beta_1$ we recover the well known result

$$G^{(\mathrm{L})}(\beta, \beta) = \begin{cases} 2\beta \ln 2 & \beta \leqslant -1 \\ (\beta - 1)\ln 2 & \beta \geqslant -1 \end{cases} \tag{68}$$

i.e. phase transition behaviour at the critical point $\beta = -1$ [12, 32, 4]. The other values in the (β_0, β_1)-plane provide us with a more detailed thermodynamic description of the system. The numerics indicates that the critical point now extends to a critical line in the (β_0, β_1)-plane. The convergence of our method is rapid. For $N = 11$ seven digits are fixed already, except at phase transition points.

Finally, returning to the general spirit of section 2, we may most generally define a path-integral transfer operator for some arbitrary (smooth) test function A depending on the entire trajectory $x_0, x_1, x_2, \ldots$ by considering a sequence of operators

$$\mathcal{L}_N[A]Q(y) = \sum_{x_0 \in f^{-N}(y)} A(x_0, x_1, \ldots, x_{N-1})Q(x_0) \tag{69}$$

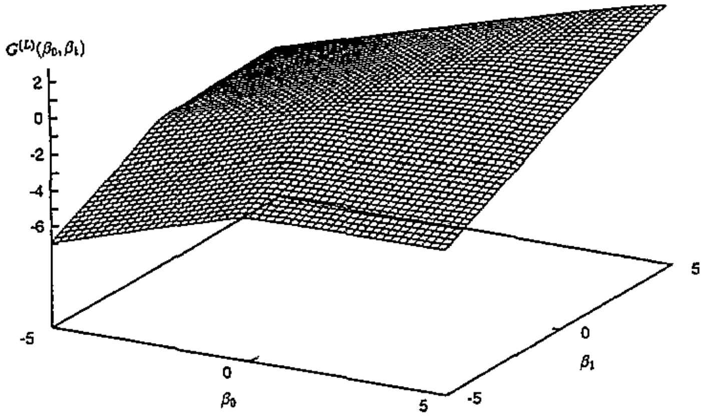

Figure 7. Thermodynamic potential $\bar{G}^{(L)}(\beta_0, \beta_1)$ of the fully developed logistic map for bivalued periodic test sequences $\beta_0, \beta_1, \beta_0, \beta_1, \ldots$, as computed from the largest eigenvalue of the 'path-integral transfer operator' $\mathcal{L}_N$.

for large N. Again one is interested in the limit $N \to \infty$ and thermodynamic potentials given by the asymptotic exponential growth rate of $\mathcal{L}_N[A]Q(y)$. The operator (65) is obtained for the special choice

$$A(x_0, \ldots, x_{N-1}) = \exp\left\{-\sum_{j=0}^{N-1} \beta_j \ln |f'(x_j)|\right\}. \tag{70}$$

8. Conclusions

In this paper we have introduced a generalized thermodynamic formalism for dynamical systems, where the observable under consideration depends on the entire trajectory of the system. In particular, the constant inverse temperature β of the usual approach is replaced by an inverse temperature field $\beta(t)$. Here t can be regarded as a relative time variable. The standard thermodynamic formalism is recovered for a constant temperature field. The partition function of our approach can be regarded as a generalized path integral, where the underlying stochastic process is not the Wiener process but a more complicated process generated by the symbolic dynamics of the mapping under consideration. Our approach generalizes the concept of Rényi entropies to entropy functionals. Similarly, the topological pressure becomes a pressure functional. A powerful tool to calculate the new thermodynamic potentials is a generalization of the transfer operator method.

An interesting application of the path-integral approach could be its use for a more general characterization of fractals. It is known that fractals and multifractals can be generated as invariant sets of one-dimensional maps [12, 20]. The dynamics on these sets is obviously transiently chaotic. One can perform a time-dependent analysis of the length scales (without normalization) induced by the generating partition of the set exactly in the same spirit as we did it with symbol probabilities in the bulk of the paper. In the case of a single-variable description ($\beta(t) \equiv$ constant), the corresponding free energy $\beta F(\beta)$ comprises all multifractal properties of the fractal set and is equivalent with the full function $D(\beta)$ of generalized dimensions. In particular, the value of the inverse temperature β where the free energy vanishes is known to coincide with the fractal dimension $D(0)$ of the set. A path-integral analysis performed with a test function $\beta_\eta(t)$ depending on some parameter η leads to a weighted average of multifractal properties over β values lying in the image range of $\beta_\eta(t)$. In particular, there may exist an η_0 where the path integral remains compensated, i.e. does neither increase nor decrease asymptotically with N. The corresponding test function β_{η_0} is then a kind of generalization of the fractal dimension concept. *In the class of test functions β_η it is β_{η_0} that tests different generalized local* dimensions $D(\beta)$ in such a way that the overall behaviour is similar to that corresponding to the fractal dimension $D(0)$.

Acknowledgments

This work has been supported by the Hungarian National Science Foundation (OTKA) under grant nos 2090, T4439, and by the International Relation Offices of Hungary and Germany, Project X231.3. It has been carried out partially in the framework of the PHARE ACCORD programme, no H9112-0378. CB also acknowledges partial support by the Deutsche Forschungsgemeinschaft during a visit to Budapest. A large part of this work was performed during CB's stay at the Institute for Theoretical Physics at the University of Aachen.

Appendix

Let us consider the case of a smooth test function $\beta(t)$. For the following it is convenient to label the matrix elements of the transfer matrix $T(\beta_n, \beta_{n-1})$ of (56) by just two indices i and j. Quite generally, the non-zero matrix elements of T are of the form $t_{ij}(\beta_n, \beta_{n-1}) = l_{ij}^{\beta_{n-1}-\beta_n} \sigma_{ij}^{\beta_n}$. Let $T^{(0)}(\beta_n, \beta_{n-1})$ denote the simplified transfer matrix obtained by formally setting all length scales l_{ij} equal to 1. The corresponding matrix elements are denoted by $t_{ij}^{(0)}(\beta_n, \beta_{n-1})$. For example, for the special case of a two-step memory map $(m = 2)$ we have

$$T(\beta_n, \beta_{n-1}) = \begin{pmatrix} \left(l_{00}^{\beta_{n-1}-\beta_n}\right)/s_{00}^{\beta_n} & \left(l_{10}^{\beta_{n-1}-\beta_n}\right)/s_{10}^{\beta_n} \\ \left(l_{01}^{\beta_{n-1}-\beta_n}\right)/s_{01}^{\beta_n} & \left(l_{11}^{\beta_{n-1}-\beta_n}\right)/s_{11}^{\beta_n} \end{pmatrix} \tag{A1}$$

and

$$T^{(0)}(\beta_n, \beta_{n-1}) = \begin{pmatrix} s_{00}^{-\beta_n} & s_{10}^{-\beta_n} \\ s_{01}^{-\beta_n} & s_{11}^{-\beta_n} \end{pmatrix} . \tag{A2}$$

In general, if we replace in (54) the transfer matrix T by the simplified transfer matrix $T^{(0)}$, the corresponding partition function is denoted by $Z_N^{(0)}$. The entropy functionals for the test function $\beta(t)$, obtained from Z_N and $Z_N^{(0)}$ in the thermodynamic limit $N \to \infty$, are denoted by $G[\beta]$ and $G^{(0)}[\beta]$, respectively.

Theorem. 1. Let $\beta(t)$ be piecewise monotonous on a finite number of intervals, and let the entries of the vectors $|a\rangle$ and $\langle c|$ be arbitrary positive numbers. Then

$$G[\beta] = G^{(0)}[\beta] . \tag{A3}$$

Proof. Let $l_{\min}$ denote the smallest length scale occurring in the transfer matrix.

$$l_{\min} = \min_{i,j} l_{ij} . \tag{A4}$$

For the moment, let us assume that $\beta(t)$ is monotonously increasing, i.e. $\beta_{n-1}-\beta_n \leqslant 0$. Thus, for any length scale l_{ij}, we have $l_{ij}^{\beta_{n-1}-\beta_n} \leqslant l_{\min}^{\beta_{n-1}-\beta_n}$. It follows

$$\begin{aligned} Z_N(\beta_0,\ldots,\beta_N) &= \langle c|T(\beta_N,\beta_{N-1})\ldots T(\beta_m,\beta_{m-1})|a\rangle \\ &= \sum_{i_{m-1},\ldots,i_N} c_{i_{m-1}} t_{i_{m-1},i_m}(\beta_{m-1},\beta_m)\ldots t_{i_{N-1},i_N}(\beta_{N-1},\beta_N) a_{i_N} \\ &\leqslant l_{\min}^{\beta_{m-1}-\beta_m}\ldots l_{\min}^{\beta_{N-1}-\beta_N} \sum_{i_{m-1},\ldots,i_N} c_{i_{m-1}} t^{(0)}_{i_{m-1},i_m}(\beta_{m-1},\beta_m)\ldots t^{(0)}_{i_{N-1},i_N}(\beta_{N-1},\beta_N) a_{i_N} \\ &= l_{\min}^{\beta_{m-1}-\beta_N} Z_N^{(0)}(\beta_0,\ldots,\beta_N)\,. \end{aligned} \tag{A5}$$

Taking the logarithm and dividing by N, the contribution of the prefactor $l_{\min}^{\beta_{m-1}-\beta_N}$ vanishes in the limit $N\to\infty$. Thus

$$\begin{aligned} G[\beta] &= -\lim_{N\to\infty}\frac{1}{N}\ln Z_N(\beta_0,\ldots,\beta_N) \\ &\geqslant -\lim_{N\to\infty}\frac{1}{N}\ln Z_N^{(0)}(\beta_0,\ldots,\beta_N) = G^{(0)}[\beta]\,. \end{aligned} \tag{A6}$$

On the other hand

$$l_{ij}^{\beta_{n-1}-\beta_n} \geqslant l_{\max}^{\beta_{n-1}-\beta_n} \tag{A7}$$

where $l_{\max}$ denotes the largest length scale occurring in the transfer matrix. Analogously we obtain from (A7)

$$G[\beta] \leqslant G^{(0)}[\beta]\,. \tag{A8}$$

Thus $G[\beta]=G^{(0)}[\beta]$ provided $\beta(t)$ is monotonously increasing. If $\beta(t)$ is monotonously decreasing, the role of $l_{\min}$ and $l_{\max}$ is exchanged. If $\beta(t)$ is just piecewise monotonous on a finite number of intervals, we can estimate the matrix elements by factors $l_{\min}^{\beta_m-\beta_{x_1}} l_{\max}^{\beta_{x_1+1}-\beta_{x_2}}\ldots$ in the regions $[\beta_m,\ldots,\beta_{x_1}],[\beta_{x_1+1},\ldots,\beta_{x_2}],\ldots$ of monotonicity, and the same proof applies, q.e.d. The extension of this result to the transfer matrix (60) containing the natural measure is straightforward.

References

[1] Alekseev V M and M V Yakobson 1981 *Phys. Rep.* **75** 287
[2] Eckmann J P and Ruelle D 1985 *Rev. Mod. Phys.* **57** 617
[3] Grassberger P 1988 *Z. Naturf.* **43a** 671
[4] Beck C and Schlögl F 1993 *Thermodynamics of Chaotic Systems* (Cambridge: Cambridge University Press)
[5] Schulman L S 1981 *Techniques and Applications of Path Integration* (New York: Wiley)
[6] Roepstorff G 1994 *Path Integral Approach to Quantum Physics* (Berlin: Springer)
[7] Simon B 1979 *Functional Integration and Quantum Physics* (New York: Academic)
[8] Ruelle D 1978 *Thermodynamic Formalism* (Reading, MA: Addison-Wesley)
[9] Sinai Ya 1972 *Russ. Math. Surveys* **166** 21
[10] Bowen R 1975 *Equilibrium States and the Ergodic Theory of Anosov Diffeomorphisms (Lecture Notes in Mathematics 470)* (New York: Springer)
[11] Collet P, Lebowitz J and Porzio A 1987 *J. Stat. Phys.* **47** 609
Arneodo A and Holschneider M 1988 *J. Stat. Phys.* **50** 995
Bessis D *et al* 1988 *J. Stat. Phys.* **51** 109
[12] Bohr T and Tél T 1988 The thermodynamics of fractals *Directions in Chaos* vol 2, ed Bai-Lin Hao (Singapore: World Scientific) pp 195–237
[13] Baladi V, Eckmann J P and Ruelle D 1989 *Nonlinearity* **2** 119
Lopes A O 1989 *SIAM J. Math. Anal.* **20** 1243
[14] Beck C 1991 *Physica* **50D** 1
[15] Rényi A 1970 *Probability Theory* (Amsterdam: North-Holland)

[16] van Kampen N G 1981 *Stochastic Processes in Physics and Chemistry* (Amsterdam: North-Holland)
[17] Kohmoto M 1987 *Phys. Rev.* A **37** 1345
[18] Tél T 1988 *Z. Naturf.* **43a** 1154
[19] Wang X J 1989 *Phys. Rev.* A **40** 6647
Fujisaka H and Inoue M 1990 *Phys. Rev.* A **41** 5302
Porzio A 1990 *J. Stat. Phys.* **58** 923
[20] Kovács Z and Tél T 1992 *Phys. Rev.* A **45** 2270
[21] Stoop R *et al* 1991 *Z. Naturf.* **46a** 642; 1991 *Physica* **50D** 405
Stoop R and Parisi J 1991 *Phys. Rev.* A **43** 1802
Stoop R 1993 *Phys. Lett.* **173A** 369; 1993 *Phys. Rev.* E **47** 3927
[22] Shigematsu H 1992 *J. Stat. Phys.* **66** 727
[23] Beck C and Graudenz D 1992 *Phys. Rev.* A **46** 6265
[24] Grossmann S and Thomae S 1977 *Z. Naturf.* **32a** 1353
[25] Thompson C J 1972 *Phase Transitions and Critical Phenomena* vol 1, ed C Domb and M S Green (London: Academic) pp 117–226
[26] Feigenbaum M J 1987 *J. Stat. Phys.* **46** 919
[27] Feigenbaum M J, Jensen M H and Procaccia I 1986 *Phys. Rev. Lett.* **57** 1503
Jensen M H and Bohr T 1987 *Phys. Rev.* A **36** 4904
[28] Szépfalusy P and Györgyi G 1986 *Phys. Rev.* A **33** 2852
[29] Csordás A and Szépfalusy P 1988 *Phys. Rev.* A **38** 2582
[30] Tél T 1990 *Directions in Chaos* ed Hao Bai-lin vol 3 (Singapore: World Scientific) pp 149–211
[31] Bohr T and Rand D 1987 *Physica* **25D** 387
[32] Tél T 1987 *Phys. Rev.* A **36** 2507
Fujisaka H and Inoue M 1987 *Prog. Theor. Phys.* **78** 268
Csordás A and Szépfalusy P 1988 *Phys. Rev.* A **38** 2582
Feigenbaum M J 1988 *J. Stat. Phys.* **52** 527
Feigenbaum M J, Procaccia I and Tél T 1989 *Phys. Rev.* A **39** 5359
Prellberg T and Slawny J 1992 *J. Stat. Phys.* **66** 503